Int J Adv Manuf Technol (2018) 95:2315–2324
https://doi.org/10.1007/s00170-017-1339-1

ORIGINAL ARTICLE

In situ chip formation analyses in micro single-lip and twist deep hole drilling

M. Kirschner[1] · S. Michel[1] · S. Berger[1] · D. Biermann[1] · J. Debus[2] · D. Braukmann[2] · M. Bayer[2]

Received: 14 July 2017 / Accepted: 7 November 2017 / Published online: 22 November 2017

Abstract Growing competitive pressure forces companies to optimise process productivity and shorten primary production times. At the same time, the resulting manufacturing quality must be kept on a high level. In the automotive sector, deep hole drilling with smallest tool diameters is an important process, e.g. to produce lubrication holes in crankshafts and fuel channels in injectors. A crucial criterion for the achievable productivity and manufacturing quality with respect to the dimensional and shape tolerances as well as the surface quality in smallest diameter deep hole drilling is the chip formation. Therefore, in-depth analyses regarding the mechanisms of chip formation at the cutting edge and the chip removal along the chip flutes are indispensable. To accomplish an in-depth chip formation analysis in smallest diameter deep hole drilling, a new methodology of analysis has been developed. Samples made of the particular test material are inserted into acrylic glass carriers, and the chip formation in the operating zone and the chip removal are documented by high-speed microscopy. In this paper, the experimental setup of the newly developed methodology of analysis and the experimental results for single-lip and twist deep hole drilling of high-strength bainitic steel with smallest diameters are shown. The investigations show the dependence of chip formation on the changes of the microstructure of the cutting edge due to tool wear, and form the basis for an optimization of the tools. In addition to that, a new approach to visualise machining processes running under non-transparent coolant is presented.

Keywords Micro machining · Single-lip deep hole drilling · Twist deep hole drilling · Chip formation

1 Introduction

In general, deep hole drilling is defined by machining processes which produce boreholes with high length-to-diameter-ratios of $l_t/D = 10\ldots400$. Even though, conventional deep hole drilling processes are used in some applications with smaller length-to-diameter-ratios $l_t/D < 10$ due to the obtainable high borehole quality [1, 2]. In this matter, deep hole drilling with tool diameters of $d \leq 2$ mm is referred to as "deep hole drilling with smallest diameters" respectively "micro deep hole drilling" [3–5]. The term "micro deep hole drilling" is not necessarily linked to the tool diameter, but rather the strictly limited and just a few micrometres counting feed rates. Because of the low feed rates, the effective rake angle differs from the nominal rake angle. This engagement situation is established as well to define micro machining [6]. Mechanical deep hole drilling with smallest diameters can be conducted by single-lip deep hole drilling (SLD) and twist deep hole drilling (TD), which are applied in a huge range of industrial sectors, e.g. automotive industry, aerospace industry, medical technology and process engineering. Figure 1 shows the fundamental drill head design of asymmetrical single-lip and symmetrical twist deep hole drills.

In consequence of the low tool rigidities, the reachable feed rates in deep hole drilling with smallest diameters are often strictly limited by growing mechanical tool loads. Long unfavourable chips must be avoided during chip formation to avoid clogging the chip flutes leading to sudden tool failure.

✉ M. Kirschner
kirschner@isf.de

[1] Institute of Machining Technology, TU Dortmund University, Baroper Straße 303, 44227 Dortmund, Germany

[2] Experimental Physics 2, TU Dortmund University, Otto-Hahn-Straße 4 a, 44227 Dortmund, Germany

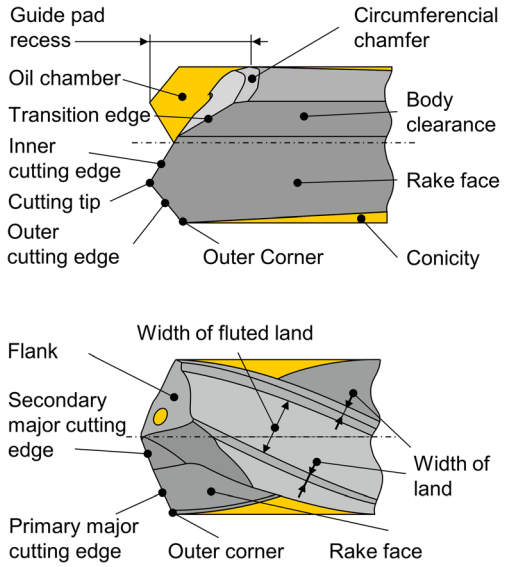

Fig. 1 Fundamental drill head design of single-lip and twist deep hole drills [5]

Feasible feed rates for difficult-to-cut materials like titanium alloys, high-strength and heat-resistant steels or nickel-based alloys like Inconel are often comparable to the cutting edge rounding (Fig. 2 left), which leads to strongly negative effective rake angles [7–9]. Although the feed rates for materials such as case-hardening and heat-treatable steels slightly exceed the cutting edge radius and thus the percentage of shear during chip formation increases (Fig. 2 right), the chip formation differs from processes in which the cutting edge rounding is negligible compared to the feed rates [5, 10]. The chip formation in front of the cutting edge rounding does not take place under the nominal rake angle in single-lip deep hole drilling of $\gamma = 0°$. This effect for micromachining processes is often referred to as the size effect [8]. In twist deep hole drilling, the chip is also not formed under the nominal rake angles varying along the primary and secondary major cutting edges or the positive rake angle of the point-thinned chisel edge.

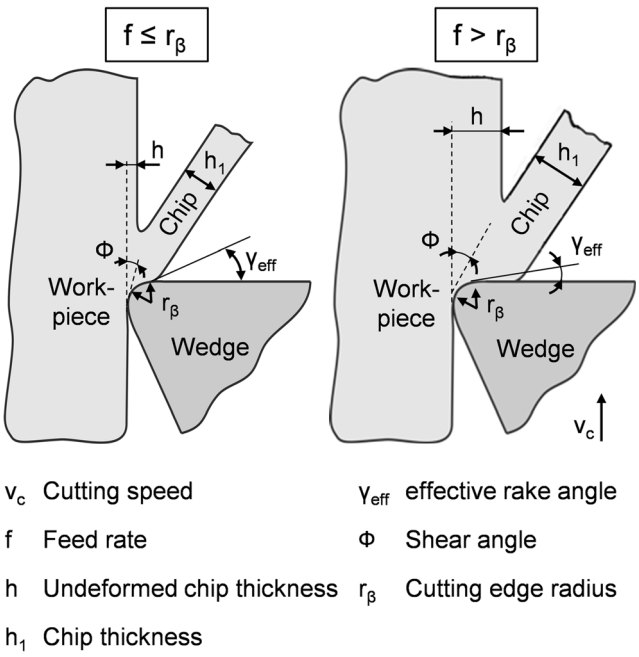

Fig. 2 Engagement situations in single-lip deep hole drilling with smallest diameters [3, 5]

The chip formation can specifically be adapted depending on the material by selecting suitable cutting speeds and feed rates as well as by different drill head designs [11, 12]. There are two different chip formation theories for single-lip deep hole drilling (Fig. 3). According to Fink's chip formation theory, two separate chips with a different curvature are formed at the inner and outer cutting edge. The chips cross each other and lead to the twisted and folded chips that are typical for single-lip deep hole drilling [12]. Heilmann observed the formation of a continuous chip over both cutting edges with the tool contour imprinted on the upper side of the chip when drilling stainless steels. In the area of the inner cutting edge, cracks occur in the chips due to the cutting speed gradient along the cutting edge [4]. Additionally to adjusting the cutting data, there are special solutions to influence the chip formation for the machining of materials that tend to form long continuous chips. By superposition the feed motion with an axial oscillation, a chip breakage can be forced. The oscillation can be generated mechanically by an axial pulsator or via piezoelectric actuators [13, 14].

In relation to the chip formation in deep hole drilling with small diameters, the ratio between the undeformed chip thickness and the cutting edge rounding is of particular importance and correlates with the resulting mechanical tool loads. Furthermore, the ratio takes a significant influence on the chip formation. A decrease in the ratio between undeformed chip thickness and cutting edge rounding results in higher chip compression [3]. The chip compression describes the relation

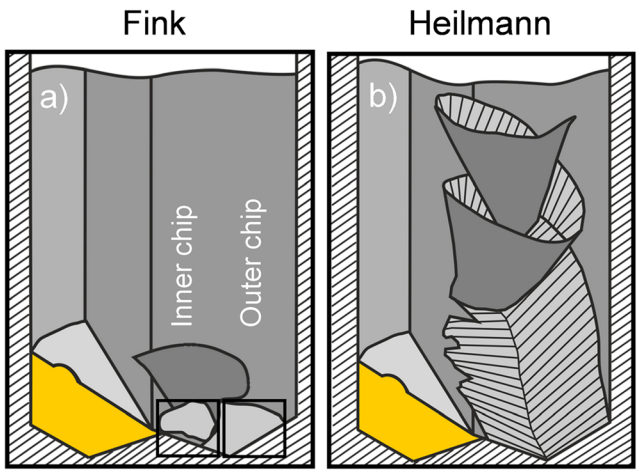

Fig. 3 Chip formation theories for single-lip deep hole drilling [4, 12]. **a** Formation of separate chips. **b** Formation of a single chip

between chip thickness and undeformed chip thickness. Beside the geometrical engagement conditions in front of the cutting edge, it is also affected by the deformability of the workpiece material and the cutting data [15, 16]. Due to the small cross sections of the chip flutes, a favourable chip formation is crucial in smallest diameter deep hole drilling. Long and disadvantageous-shaped chips can lead to chip jamming in the chip flute. Consequently, the chip evacuation is interrupted and sudden tool failures occur. Furthermore, the surface quality of the boreholes is reduced due to the scratching of the chips. The chip formation strongly relates to the choice of the cutting data and to the macroscopic point geometry of the tool. In single-lip deep hole drilling, standard point geometries are characterised by a tipped point design, divided in an inner and outer cutting edge with angles of $K_1 = 50 \ldots 70°$ and $K_2 = 105 \ldots 120°$ [1]. To improve the productivity by specifically influencing the chip formation, a range of special point designs have been developed. The special point designs distinguish themselves by a third middle cutting edge, a bowed outer cutting edge or a positive rake angle, which is created by a chip former on the rake face [5, 9, 11]. In twist deep hole drilling, the chip flow direction and curvature are affected in particular by the major cutting edge design (convex, straight or concave) and the helix angle of the chip flutes. Moreover, a cooling lubricant is supplied through cooling channels inside the tool shank, to support the chip evacuation along the chip flutes and to reduce the tool wear at the cutting edges and the contact elements on the circumference of the tool. In general, decreasing tool diameters and increasing length-to-diameter-ratios to be machined require higher cooling lubricant pressures.

Up to now, one of the major restrictions in drilling processes, especially in micro deep hole drilling, lies in the chip formation, respectively, the chip evacuation. The widespread method of using quick-stop devices is not feasible for analysing the chip formation and the interaction between workpiece, chip and tool in smallest diameter deep hole drilling due to the impracticable demands on sudden acceleration and abrupt separation of tool and workpiece [17]. The newly developed method of high-speed chip formation analysis uses transparent acrylic glass carriers to enable the visualisation and documentation of the chip formation during the drilling process [18]. The method gives important insights in the formation of chips, the interaction of the chip, the tool surfaces and the cooling lubricant, as well as the development of the chip formation with increasing drilling paths. The knowledge gained can be used for the further development and optimization of tool designs, the improvement of coating systems and the adaptation of process parameters to the specific material to be machined. The focus of the experiments in this article is on the investigation of single-lip deep hole drills. On the basis of the examination of twist drills, the transferability of the analytical method to other tool concepts will be tested.

2 Experimental setup

In general, drilling processes take place in a closed operating zone surrounded by workpiece material. To visualise and analyse the chip formation in deep hole drilling with smallest tool diameters, the non-transparent workpiece material was substituted by transparent acrylic glass [18]. The experimental setup for the high-speed chip formation analyses was integrated into a one spindle deep hole drilling machine from TBT Tiefbohrtechnik GmbH of type ML-200. The machine tool is specially designed for deep hole drilling in the diameter range of $d = 0.5 \ldots 6$ mm. The machine's high-frequency spindle allows high rotational speeds up to $n_{max} = 36{,}000\ \mathrm{min}^{-1}$. Furthermore, a high-pressure pump can realise lubricant pressures up to $p_L = 230$ bar. The lubricant used is a mineral oil with a kinetic viscosity of $\nu = 10\ \mathrm{mm}^2/\mathrm{s}$ (40 °C). The machine tool allows machining with a rotating tool and a stationary workpiece as well as machining with a rotating tool and an inversely rotating workpiece. In the last-mentioned working method characterised by inversely relative movement between tool and workpiece, a tailstock is used to rotate the workpiece. While deep hole drilling with rotating tool and stationary workpiece, the workpiece to be machined is mounted on an NC-cross table. In addition to the *Z*-axis for positioning the high-frequency spindle, the three axes (*X*, *Y*, *W*) of the cross table allow a flexible positioning of the workpiece.

To enable a constant view on the rake face and to continuously monitor the chip formation as well as the chip evacuation, it is indispensable to work with a stationary deep hole drilling tool and a rotating workpiece. Therefore, the functions of the high-frequency spindle and the NC-cross table have to be reversed in the high-speed analyses. For this purpose, the feed motion is realised on the tool side by the NC-cross table. The deep hole drilling tool is connected to the NC-cross table by a dynamometer, a specially manufactured adapter, a tool holder, an adjustment sleeve and a collet chuck. Furthermore, a trigger between the recording device and the high-speed camera allows a synchronous measuring of the mechanical loads. The specially manufactured adapter is used on the one hand to connect the dynamometer with the NC-cross table and on the other hand to enable the lubricant supply while working with the inverted experimental setup. The adapter offers the possibility of working with different lubrication concepts, e.g. internal high-pressure cooling, minimum quantity lubrication or cryogenic cooling. For the experimental investigations described in this paper, the lubrication concept used by default, internal high-pressure cooling was supplied for the analyses on the high-strength bainitic steel. Therefore, the mineral oil stored in the integrated machine tank is redirected by high-pressure hoses from the high-pressure pump to the adapter. The transparent acrylic glass carriers with the workpiece material inside are mounted in the high-frequency spindle with a special collet chuck holder. To minimise concentricity errors,

the carriers are supported by a clamping cone, which is mounted in the chip chamber. The opening angle of the clamping cone measures 60° with a diameter corresponding to the outer diameter of the acrylic glass carriers. Because of the double-sided mounting of the acrylic glass carriers and the immersion of the tool holder in a special housing that is mounted in the chip chamber, the process is completely sealed. Thus, the return flow of the cooling lubricant is guided through the chip chamber and it is possible to collect the produced chips for subsequent investigations.

In the experimental setup, the high-speed camera is positioned orthogonally to the rotating acrylic glass carriers between the clamping cone and the collet chuck holder. To connect the feed motion of the cutting tools to the focus of the high-speed camera, the camera is attached to the cross table by an adjustable camera holder. Additionally, the tool area to be analysed can precisely be adjusted by a fine adjustment of the high-speed camera and by the setting angle of the tool. Figure 4 shows the experimental setup.

To carry out the analyses, the acrylic glass carrier with the workpiece inside is clamped in the collet chuck holder first. Afterwards, the high-frequency spindle is moved towards the clamping cone until the acrylic glass carrier fits to the mounted

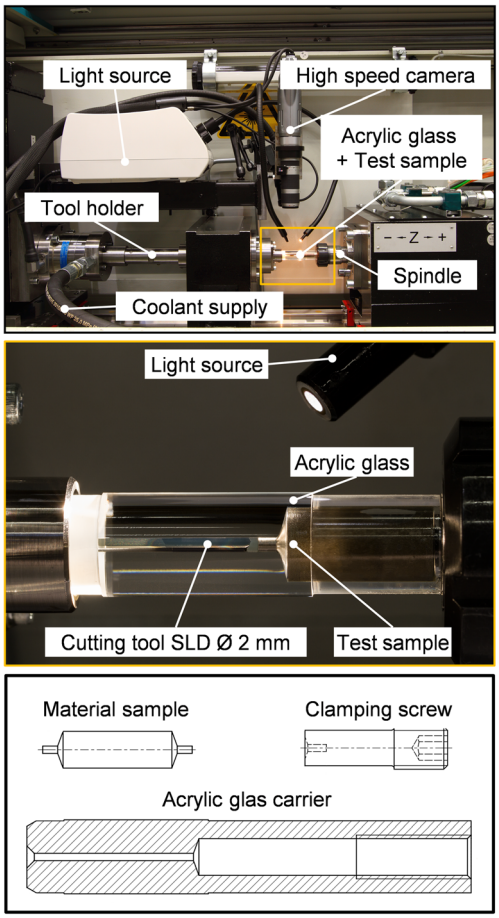

Fig. 4 Experimental setup of the high-speed chip formation analyses

cone. In the next step, the non-rotating cutting tool is inserted into the guide bore in the acrylic glass carrier and subsequently adjusted to the high-speed camera focus. The bore hole in the acrylic glass is matched to the tool diameter and has narrow tolerances in order to ensure optimum guidance of the tool and to prevent the tool from being pushed off when the cutting edges enter the workpiece. Due to the limited feed rates, only relatively low radial forces are generated during drilling with smallest diameters. The single-lip deep hole drills with the circumferential form G have a large contact surface to the bore hole wall via the guide pad with a contact angle of 120° and thus generate a very low surface pressure on the acrylic glass surface. Only marginal deformations occur, so that the substitution of the bore wall with acrylic glass has a negligible influence on chip formation and the drilling process. During chip removal, scratches can occur in the acrylic glass, so that an influence of the acrylic glass on the chip transport cannot be completely excluded. However, the focus of the investigations carried out is on chip formation at the cutting edges of the tools. The workpieces made of the bainitic steel 20MnCrMo7 with a tensile strength of Rm = 1260 MPa are drilled over a length of about 3 mm. Meanwhile, the high-speed camera records all stages of deep hole drilling from the first cut to the stationary drilling process where the whole cutting edge is engaged. Furthermore, it is possible to gain knowledge about the chip removal along the chip flute. Because of the low feed rates per revolution during deep hole drilling with smallest diameters, there are several chip formations visible in one analysis that can be evaluated. For this reason, it is not necessary to repeat each analysis to statistically verify the experiments. Before the start of the high-speed chip formation analyses, the respective process parameters are adjusted and the measuring chain is configured. The chip formation processes were recorded by the high-speed camera KEYENCE VW-9000 at a frame rate of 10,000 fps and an exposure time of 1/20,000 s.

To illuminate the various functional surfaces of the single-lip and twist deep hole drills, it is necessary to use a number of light sources. Therefore, several cold-light sources have been used. Nevertheless, the chip formation cannot be analysed and documented by high-speed microscopy, when using cold-light sources and simultaneously adjusting high coolant pressures. The enhanced coolant pressure leads to heavy turbulences in the lubricant and the cold-light is refracted at the interfaces between liquid and air inclusions. Consequently, the use of cold-light sources in the analyses requires a reduced lubricant pressure. An unrestricted transparency exists when adjusting a reduced lubricant pressure of $p_L = 40$ bar. Within this matter, pre-analyses proved that the chip formation is not changed significantly with increasing coolant pressure (Fig. 5).

However, the coolant and chip velocity within the chip removal is accelerated at higher pressures. The chip velocity is proportional to the lubricant volume flow of the

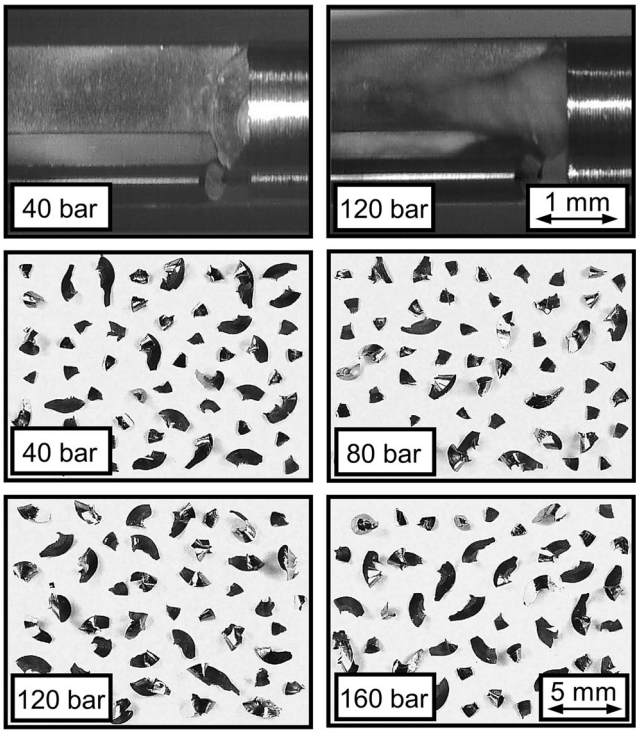

Fig. 5 Influence of the cooling pressure on the transparency of the coolant and the chip formation

SLD	Geometry
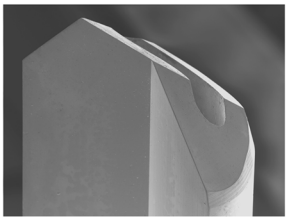	Ø = 2.0 mm
	κ_1 = 50°; κ_2 = 120°
	Circumferential Shape G
	AlTiN coating

TD	Geometry
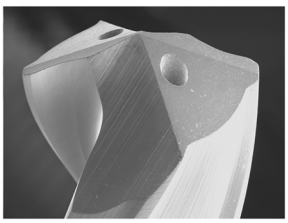	Ø = 2.0 mm
	σ = 135°
	γ_t = 30°
	TiAlN-TiSiN coating

Fig. 6 Specifications of the single-lip and twist deep hole drills used in the analyses

standardised single-lip deep hole drill with a tool diameter of $d = 2.0$ mm, which counts approximately $\dot{V} = 0.08$ l/min at a coolant pressure of $p_L = 40$ bar compared to $\dot{V} = 2.0$ l/min at $p_L = 120$ bar. To visualise the high-speed chip formation and to conduct the analyses under high coolant pressures, a new approach using laser diodes with specific emission wavelength to illuminate the working area is tested. The electromagnetic radiation selected is characterised by a high transmission degree, and thus, reflections in the lubricant's turbulences are supressed. In the experiments, single-lip and twist deep hole drills with a tool diameter of $d = 2.0$ mm, designed for the machining of holes with a length-to-diameter ratio $l_t/D = 30$, have been used (Fig. 6). The tool shank is made of solid cemented carbide in both tool concepts. The AlTiN-coated single-lip deep hole drills have a standard point geometry with angles of the outer and inner cutting edge of $K_1 = 50°$ and $K_2 = 120°$. In addition, twist deep hole drills with a concave primary major cutting edge, a straight secondary major cutting edge, a point angle of $\sigma = 135°$, a helix angle of $\gamma_t = 30°$ and a TiAlN-TiSiN coating were used. In the initial state, all tools have an average cutting edge rounding of $r_\beta = 5…8$ µm.

3 High-speed analyses on single-lip deep hole drilling

The single-lip deep hole drilling of the high-strength bainitic steel 20MnCrMo7 was conducted with a cutting speed of $v_c =$ 70 m/min and a feed rate of $f = 20$ µm. The created image sequence of the high-speed chip formation analysis in Fig. 7 shows that the chip formation takes place over the entire cutting width. Using the standard point geometry in an unworn state, the chip forms on the inner and outer cutting edge and curves as a result of the cutting speed gradient over the radius of the tool immediately in the direction of the tool centre.

At the drill axis, the direction of the chip is perpendicular to the feed direction (t_1). The outline of the cutting edge and the track of the cutting tip are visible on the topside of the chip. The chip curls across the rake face and the transition edge in the direction of the previously produced bottom of the borehole (t_2). When it hits the base of the rotating material sample, the chip bends above the transition edge and breaks due to the forward flow of the material (t_3). The fractured discontinuous chips can be removed free from interferences along the axial slot of the tool and ensure a high process stability (t_4).

Parallel to the high-speed chip formation analyses, tests were performed on single-lip deep hole drilling in block material of 20MnCrMo7. The shape of the produced chips at the beginning of the deep hole drilling process resembles the chips observed in the high-speed chip formation analysis in Fig. 7. But, over the drilling path, the chip formation changes significantly (Fig. 8). The length of the chips increases with the drilling path. After a drilling distance of $l_f = 10{,}000$ mm, highly deformed, concertina-shaped chips are formed, which reduce the process stability and can easily jam between the borehole wall and the chip flute of the tool. The chip lengths can reach up to $l_{Ch} = 10.1$ mm.

The fundamentally altered chip formation after a drilling path of $l_f = 10{,}000$ mm can also be observed in the

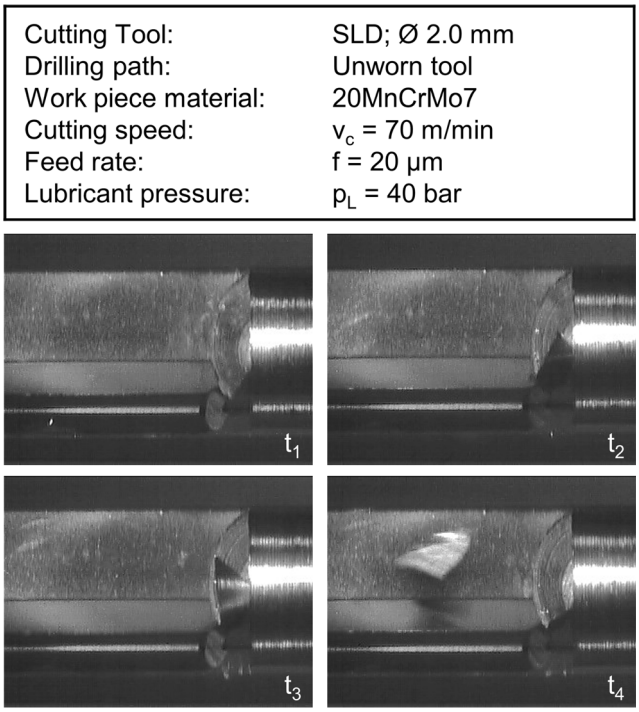

Fig. 7 Chip formation in SLD of 20MnCrMo7 at the beginning of the process

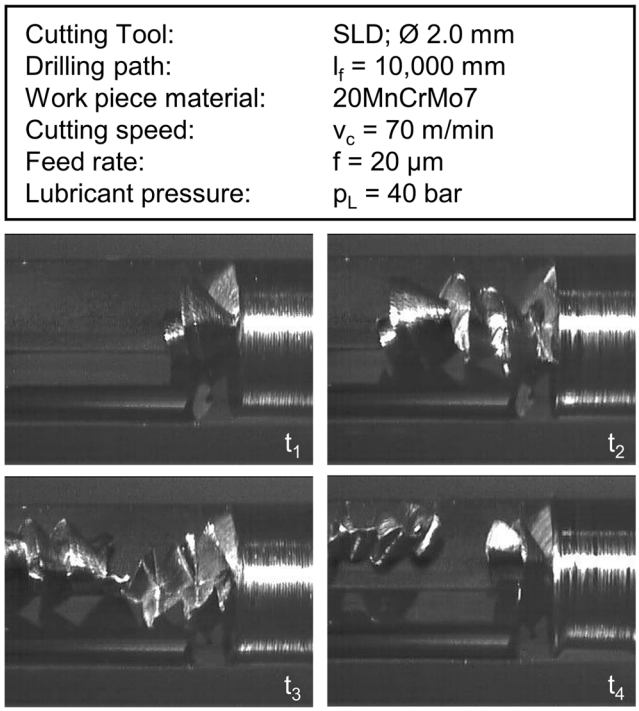

Fig. 9 Chip formation in SLD of 20MnCrMo7 after a feed travel of l_f = 10,000 mm

high-speed chip formation analysis (Fig. 9). As a result of the higher flow velocity at the outer cutting edge, the chip also curves in the direction of the tool centre (t_1). Compared to a new tool, however, the contact between the chip and the back of chip flute causes the chip to form a helix before developing folded concertina-shaped chips. The continuous chip is repeatedly pushed against the transition edge, bends and forms a folded structure ($t_{2–3}$). After a large number of bends, the chip is separated by the cooling lubricant (t_4).

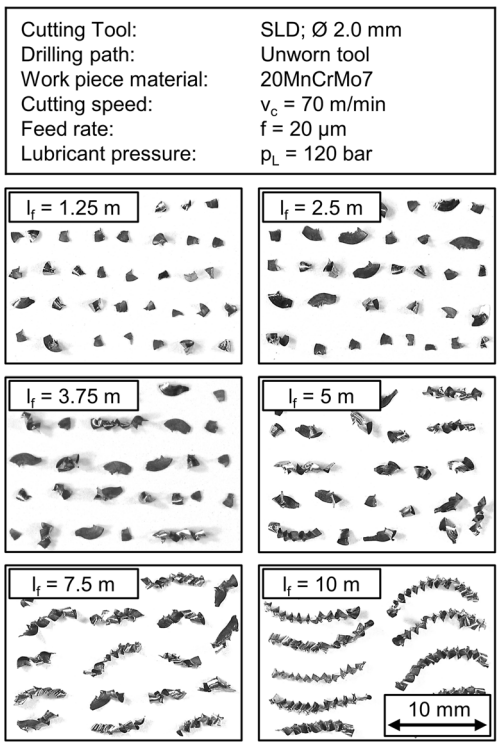

Fig. 8 Development of the chip formation with increasing drilling path

A detailed view at the tool wear provides an explanation for the significant changes in the chip formation with an increasing drilling path. Figure 10 shows energy-dispersive X-ray spectroscopy (EDX) and height profiles of the rake face, analysed by confocal white light microscopy, of new and worn single-lip deep hole drills with standard geometry.

A single-lip deep hole drill in the initial state produces discontinuous chips and has an intact coating in the area of the cutting edges. However, with a growing drilling path, a significant build-up edge is formed on the rake face supported by the ability of the bainitic steel to cold-hardening, the stable and largely stationary chip formation, the stagnation zone in the material flow in front of the cutting edge and the sufficiently low temperatures in the chip formation zone suppressing a recrystallisation of the material [15, 19]. The energy-dispersive X-ray spectroscopy of the cutting edge after a drilling path of l_f = 10,000 mm shows the abraded tool coating, the cutting edge rounding and the build-up edge with a height of h_a = 26 µm adhesively formed on the carbide substrate. By means of confocal white light microscopy, the formation of the build-up edge can be analysed over the drilling path. In this case, the build-up edge increases continuously over the drilling path of l_f = 10,000 mm and is not

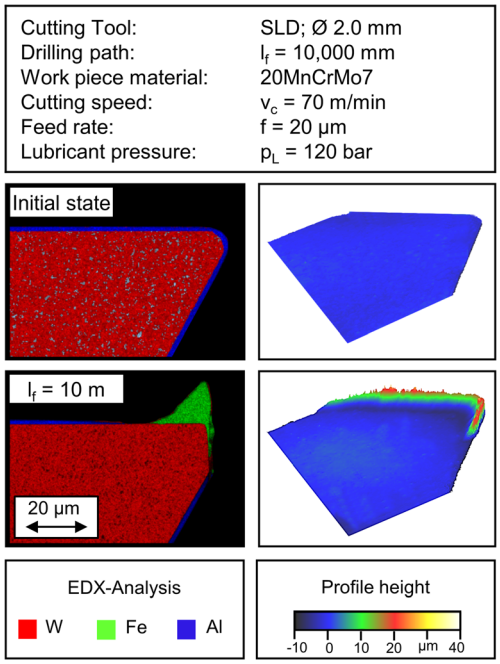

Fig. 10 Tool wear in SLD of 20MnCrMo7

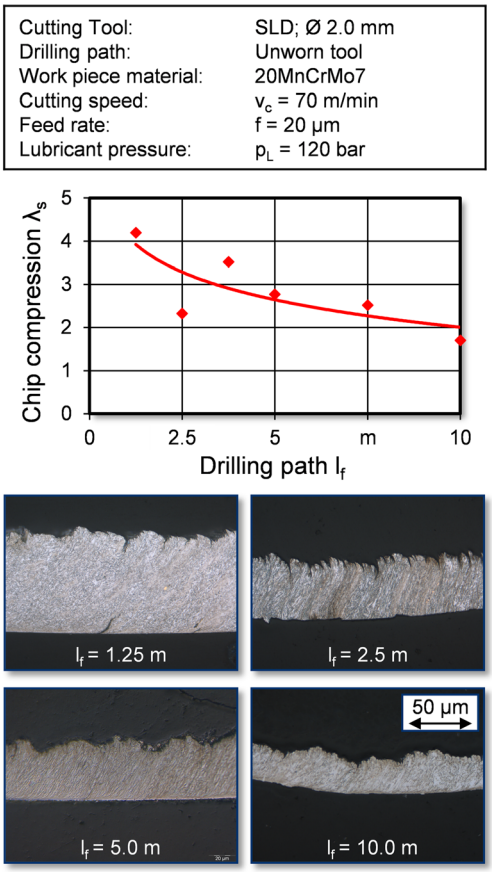

Fig. 11 Chip compression in SLD of 20MnCrMo7

characterised by a regular build-up and breakdown. The formation of the build-up edge and the abrasive wear completely change the cutting edge geometry with increasing cutting path and thus the engagement conditions of the tool in the single-lip deep hole drilling process. In the new state, the cutting edge rounding measured at the outer and inner cutting edge was $r_ß = 7.8$ µm. At a feed rate of $f = 20$ µm, the chip formation partially took place in front of the cutting edge rounding and on the rake face. The nominal rake angle of $\gamma_{nom} = 0°$ is characteristic for single-lip deep hole drilling. Overall, an effective rake angle of $\gamma_{eff} \leq 0°$ is thus obtained. Using a confocal white light microscope, digitised height profiles are evaluated at different positions along the cutting edge and the average rake angles are determined. After a drilling path of $l_f = 5000$ mm, the effective rake angle is positive and amounts to $\gamma_{eff} = 20°$. The rake angle increases further, reaching $\gamma_{eff} = 28°$ at a drilling path of $l_f = 10{,}000$ mm, which leads to a strong decrease in the chip compression.

The chip compression was calculated on the basis of the undeformed chip thickness and the chip thickness determined in cross sections of the collected chips. The measurement of the chip thickness was carried out in the area of the cutting tip, where the angle of incidence is approximately $K = 90°$. The undeformed chip thickness thereby equals the feed and could be assumed to be constant at $h = f = 20$ µm. Figure 11 shows the cross sections of the chips after different drilling paths and the development of the chip compression. While at a drilling path of $l_f = 1.25$ m the chip compression counts $\lambda_s = 4.2$, the value decreases with the development of the build-up edge and the resulting increase of the effective rake angle to $\lambda_s =$ 1.7 at a drilling path of $l_f = 10$ m. Due to the lower compression of the material, there is no chip breakage and long unfavourable chips are produced.

4 High-speed analyses on twist deep hole drilling

Moreover, analyses on twist deep hole drilling of high-strength bainitic steel 20MnCrMo7 with smallest diameters have been carried out. In a first step, the feasibility of twist deep hole drilling with a length to diameter ratio of $l_t/D = 30$ in block material has been checked. A cutting speed of $v_c = 80$ m/min and a feed rate of $f = 50$ µm have been selected, so that the productivity is roughly tripled compared to single-lip deep hole drilling. However, a process adaption was necessary to realise twist deep hole drilling. When adjusting lubricant pressures of $p_L = 100$ bar, the process stability is insufficient and tool failures occur in higher drilling depth. The chip formation can be described as favourable, but problems exist during the chip evacuation. A lubricant pressure of $p_L = 100$ bar and thus a lubricant flow rate of $\dot{V} = 0.085$ l/min results in a high chip removal velocity in the limited cross sections of the chip flutes. In enhanced drilling depth, the chip evacuation in

twist deep hole drilling becomes increasingly difficult and chips are pushed on each other in the twisted chip flutes. Consequently, clogging in the chip flutes takes place (Fig. 12), which can also be observed in a large increase in the drilling torque.

To reduce the process disturbances, the lubricant pressure has been adjusted. A lubricant pressure of $p_L = 40$ bar leads to a significant decrease in the lubricant flow rate ($\dot{V} = 0.2$ l/min) and the chip removal velocity. As a result, the chips are evacuated undisturbedly, exclusively by the rotation of the twisted chip flutes according to the conveying principle of an Archimedean screw. However, a small lubricant flow rate provides a sufficient lubrication to the cutting edges and the contact elements. The chip formation does not depend on the lubricant flow rate. The production of chips in twist deep hole drilling has been analysed by high-speed chip formation analyses in the second step (Fig. 13).

In twist deep hole drilling, tightly curved chip curls are produced along the primary and secondary major cutting edge (t_{1-2}). The rake angle and the radius of the chip flute profile define the curvature radius of the chip curls. The separation is initiated by the impact on the chip flute (t_3). Afterwards, the chip curls are removed along the twisted chip flutes (t_4). Due to the small cross sections of the chip flutes, the chips contact the bore hole surface, which can be observed as scratch marks on the acrylic glass. In contradiction to single-lip deep hole drilling of 20MnCrMo7 with smallest diameters, the chip formation is not be changed over the drilling path due to the increased undeformed chip thicknesses and the varying engagement situation and cutting forces.

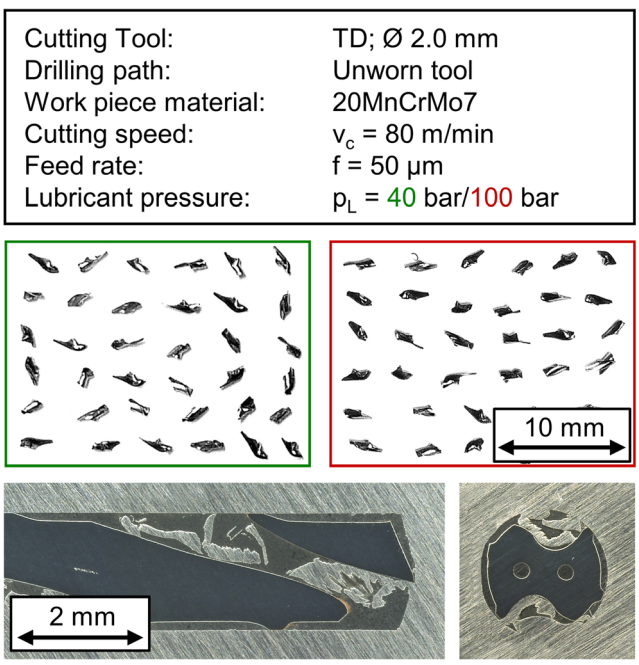

Fig. 12 Correlation between chip formation and lubricant pressure in TD

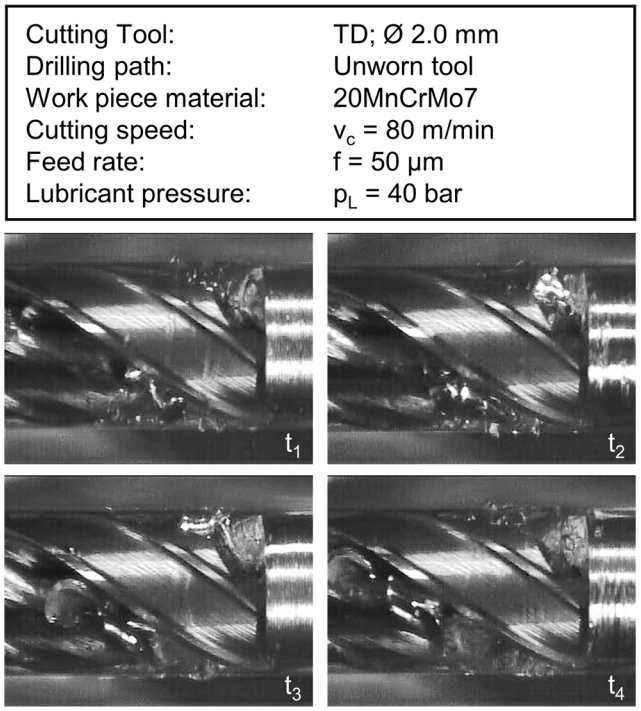

Fig. 13 Chip formation in TD of 20MnCrMo7 at the beginning of the process

5 Illumination with specific laser diodes

In addition to the experiments with cold-light sources, an experimental setup based on selective wavelength-illumination for high-speed chip formation analyses with extended lubricant pressure has been investigated. For this purpose, five laser diodes with specific emission wavelength have been used to illuminate the working area. The laser diodes are mounted in self-manufactured, cylindrical fixtures made of aluminium and are positioned around the operating zone by flexible magnetic stands. An internal air cooling of the cylindrical fixtures protects the laser diodes from overheating. To collimate the laser beams, collimation tubes with aspheric lenses having antireflection coatings for the near-infrared spectral range are adapted in front of each laser diode (Fig. 14).

In preliminary tests, the wavelength of the required electromagnetic radiation that has a high transmission degree through the lubricant was identified to reduce the reflections in the lubricant's turbulences. Therefore, a transmittance spectrum was recorded by a BRUKER Vertex 80v Fourier transform infrared (FTIR) spectrometer. Figure 15 shows the transmittance spectrum recorded for the deep hole drilling oil used in the experiments.

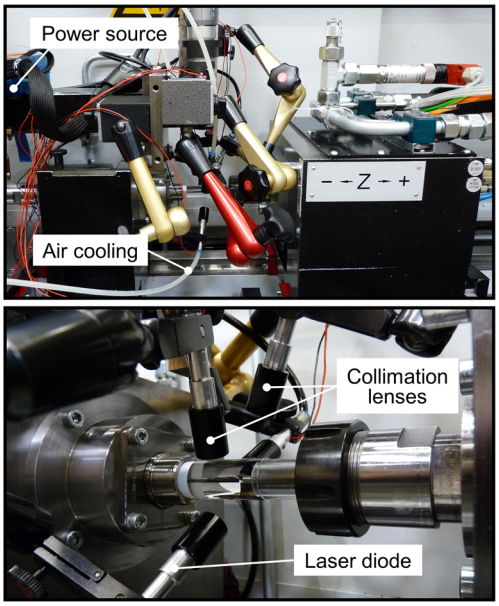

Fig. 14 Illumination of the operating zone with specific laser diodes

The minimum absorption of the mineral deep drilling oil was found at $\lambda_l = 852$ nm. For this reason, five THORLABS laser diodes with a typical centre wavelength of $\lambda_l = 852$ nm and an optical power of $P_o = 100$ mW were used to illuminate the working area in the high-speed chip formation analyses with extended lubricant pressure. Moreover, the detection efficiency of the high-speed camera is high for emission wavelengths around 850 nm. In Fig. 16, the transparency degree when illuminating the working zone with cold-light sources and laser diodes in single-lip deep hole drilling with a coolant pressure of $p_L = 120$ bar is compared.

The usage of specific laser diodes offers a possibility to improve the visibility of the chip formation under high lubricant pressures. Nevertheless, the recordings of the initial analyses are characterised by image noise by means of interference effects. In prospective analyses, the positioning of the laser diodes shall be arranged more systematically in order to reduce the image noise and, in turn, to enhance the image quality. Thus, the image noise will be reduced and the image quality enhanced.

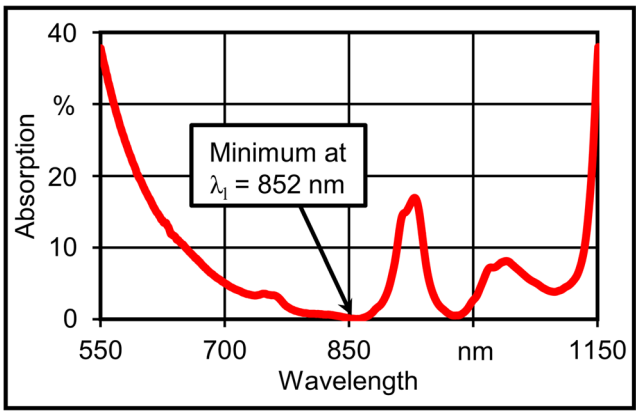

Fig. 15 Transmittance spectrum of the deep drilling oil used in the experiments

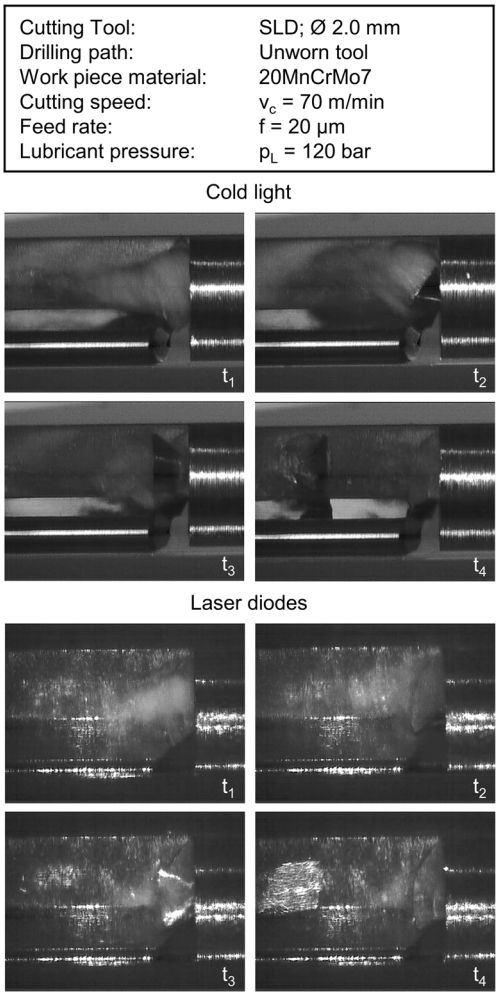

Fig. 16 High-speed chip formation analyses under high lubricant pressure

6 Conclusion

Because of the closed operating zone in deep hole drilling, the chip formation and evacuation are very challenging. Even more difficult becomes the chip removal in deep hole drilling with smallest tool diameters due to the strictly limited cross sections of the chip flutes. To analyse the important chip formation in deep hole drilling with smallest diameters, a new methodology has been developed. In the high-speed chip formation analyses, transparent acrylic glass carriers with inserted test material samples are used to visualise and analyse the chip formation and evacuation. The substitution of the surrounding, non-transparent workpiece material by transparent acrylic glass allows recording all stages of the chip formation by high-speed microscopy in real time. In this paper, the experimental setup integrated into a conventional deep hole

drilling machine as well as results of high-speed chip formation analyses on single-lip deep hole drilling with a tool diameter of $d = 2.0$ mm of the high-strength bainitic steel 20MnCrMo7 are presented. Experiments with twist deep hole drills show the transferability of the new analysis technique. The analyses on single-lip deep hole drilling emphasise the significant change of the chip formation with increasing drilling path. After the abrasive removal of the tool, coating a built-up edge on the uncovered cemented carbide is formed at the cutting edges. The built-up edge leads to a complete change of the engagement situation with respect to the effective rake angle. The results on micro single-lip deep hole drilling of the bainitic steel 20MnCrMo7 show that the change in the chip formation correlates with the tool wear. As a result of a lower chip compression, unfavourable chips are produced that considerably reduce the process stability. Based on the detailed analyses, modifications regarding the tool design, tool coating, process strategy etc. can be derived by tool manufacturers to improve the tools and thus the productivity of deep hole drilling processes with small diameters. In conclusion, the analyses provide important insides into the process restrictions regarding the tool life in single-lip deep hole drilling of high-strength steels with smallest diameters. Moreover, the high-speed analyses on twist deep hole drilling demonstrate very clearly the chip formation and separation of the representative chip curls. While conducting all high-speed chip formation analyses under lubricant supply, problems in terms of turbulences and restricted transparency occur when adjusting enhanced lubricant pressures. For this reason, a new approach using laser diodes with specific wavelengths to illuminate the operating zone is presented to study deep hole drilling processes with high lubricant pressures in future.

Funding information The authors would like to thank the German Research Foundation (DFG) for funding the project BI 498/67 “High-speed analysis of the chip formation in small diameter deep hole drilling of high-strength and difficult-to-machine materials”.

References

1. VDI-Richtlinie 3208 (2014) Tiefbohren mit Einlippenbohrern. Beuth-Verlag, Berlin
2. VDI-Richtlinie 3210 (2006) Tiefbohrverfahren. Beuth-Verlag, Berlin
3. Eichler R (1996) Prozeßsicherheit beim Einlippentiefbohren mit kleinen Durchmessern. Universität Stuttgart, Dissertation
4. Heilmann M (2012) Tiefbohren mit kleinen Durchmessern durch mechanische und thermische Verfahren. Technische Universität Dortmund, Dissertation
5. Kirschner M (2016) Tiefbohren von hochfesten und schwer zerspanbaren Werkstoffen mit kleinsten Durchmessern. Technische Universität Dortmund, Dissertation
6. Denkena B, Biermann D (2014) Cutting edge geometries. CIRP Ann Manuf Technol 63(2):631–653. https://doi.org/10.1016/j.cirp.2014.05.009
7. Okasha MM, Mativenga PT, Li L (2011) Sequential laser mechanical microdrilling of Inconel 718 alloy. J Manuf Sci Eng 133(1): 011008. https://doi.org/10.1115/1.4003334
8. Imran M, Mativenga PT, Kannan S, Novovic D (2008) An experimental investigation of deep hole microdrilling capability for a nickel-based superalloy. J Eng Manuf 222(12):1589–1596. https://doi.org/10.1243/09544054JEM1217
9. Biermann D, Kirschner M (2015) Experimental investigations on single-lip deep hole drilling of superalloy Inconel 718 with small diameters. J Manufacturing Processes, 20 1:332–339
10. Heisel U, Stortchak M, Eisseler R (2003) Determination of cutting parameters in deep hole drilling with single-fluted gun drill of smallest diameters. Prod Eng X(/1):51–54
11. Zabel A, Heilmann M (2012) Deep hole drilling using tools with small diameters—process analysis and process design. CIRP Annals–Manufacturing Technol, 61(1):111–114. https://doi.org/10.1016/j.cirp.2012.03.002
12. Fink PG (1977) Zerspanungsuntersuchungen zur Verbesserung der Spanabführung, der Bohrungsqualität sowie der Wirtschaftlichkeit beim Tiefbohren mit Einlippen-Werkzeugen. Universität Stuttgart, Dissertation
13. Heisel U, Wallaschek J, Eisseler R, Potthast C (2008) Ultrasonic deep hole drilling in electrolytic copper ECu 57. CIRP Annals–Manufacturing Technol 57(1):53–56. https://doi.org/10.1016/j.cirp.2008.03.078
14. Schur S (2008) Mit axialem Pulsieren zu höherem Vorschub–Hochleistungs-Tiefbohren mit dem Axial-Pulsator. Werkstatt und Betrieb 4:2–4
15. B. Denkena, H. K. Tönshoff: Spanen–Grundlagen. Springer Verlag, 3. Auflage, Heidelberg, (2011)
16. Klocke F, König W (2008) Fertigungsverfahren–Drehen, Fräsen, Bohren. 8. Auflage. Springer-Verlag, Heidelberg
17. Griffiths BJ (1986) The development of a quick-stop device for use in metal cutting hole manufacturing processes. Int J Machine Tool Design Res, 26(2):191–203. https://doi.org/10.1016/0020-7357(86)90219-2
18. Biermann D, Kirschner M, Eberhardt D (2014) A novel method for chip formation analyses in deep hole drilling with small diameters. Production Engineering–Res Developments, 8(4):491–497. https://doi.org/10.1007/s11740-014-0566-7
19. H. Opitz: Die Aufbauschneidenbildung bei der spanabhebenden Bearbeitung. Westdeutscher Verlag, Köln und Opladen, (1964), https://doi.org/10.1007/978-3-322-98657-3